



DNA-only, microwell-based bioassay for multiplex nucleic acid detection with single base-pair resolution using MNazymes

Saba Safdar^{a,1}, Karen Ven^{a,1}, Julie van Lent^a, Benjamin Pavie^b, Iene Rutten^a, Annelies Dillen^a, Sebastian Munck^b, Jeroen Lammertyn^{a,*}, Dragana Spasic^a

^a Department of Biosystems, Biosensors Group, KU Leuven, 3001, Leuven, Belgium

^b VIB-KU Leuven Center for Brain & Disease Research, KU Leuven, 3000, Leuven, Belgium

ARTICLE INFO

Keywords:

MNAzyme
Multiplex bioassay
Mutation
Diagnostics
Protein-free
Nasopharyngeal swab samples

ABSTRACT

In disease diagnostics, single- and multiplex nucleic acid (NA) detection, with the potential to discriminate mutated strands, is of paramount importance. Current techniques that rely on target amplification or protein-enzyme based signal amplification are highly relevant, yet still plagued by diverse drawbacks including erroneous target amplification, and the limited stability of protein enzymes. As a solution, we present a multicomponent nucleic acid enzymes (MNAzymes)-based system for singleplex and multiplex detection of NA targets in microwells down to femtomolar (fM) concentrations, without the need for any target amplification or protein enzymes, while operating at room temperature and with single base-pair resolution. After successful validation of the MNAzymes in solution, their performance was further verified on beads in bulk and in femtoliter-sized microwells. The latter is not only a highly simplified system compared to previous microwell-based bioassays but, with the detection limit of 180 fM, it is to-date the most sensitive NAzyme-mediated, bead-based approach, that does not rely on target amplification or any additional signal amplification strategies. Furthermore, we demonstrated, for the first time, multiplexed target detection in microwells, both from buffer and nasopharyngeal swab samples, and presented superior single base-pair resolution of this assay. Because of the design flexibility of MNAzymes and direct demonstration in swab samples, this system holds great promise for multiplexed detection in other clinically relevant matrices without the need for any additional NA or protein components. Moreover, these findings open up the potential for the development of next-generation, protein-free diagnostic tools, including digital assays with single-molecule resolution.

1. Introduction

Nucleic acid (NA) detection is a hallmark and an essential aspect of disease diagnostics as it allows detection of genetic material of, for example, pathogenic microorganisms (e.g. bacteria (de Abreu Fonseca et al., 2006; Warwick et al., 2004) and viruses (Abe et al., 1999; Schneider et al., 1985)) and tumor cells (Han et al., 2017). As such, it is pivotal for guiding a timely therapeutic intervention and for combatting antimicrobial resistance, among other applications. Due to evolution in diagnostics, now information is sought on more than just the presence of the target and its concentration. The occurrence of mutations or other confounding target sequences in the same sample are examples of a few parameters that are essential for the future development of diagnostics.

The majority of current methods used to achieve these aims still rely

on target amplification, such as the gold standard real-time quantitative polymerase chain reaction (Heim et al., 2003), or the more recent isothermal amplification approaches, including rolling circle amplification (Kühnemund et al., 2017), loop-mediated isothermal amplification (Kishine, 2014), and helicase-dependent amplification (Vincent et al., 2004). In spite of their indisputable relevance, target amplification approaches involve several drawbacks, most notably the high chances of erroneous sequence amplification, which result in an accumulation of false-positive results (Borst et al., 2004). In this context, novel approaches have been reported, relying on direct detection of the target strands rather than amplification thereof. Here, target detection is achieved through hybridization with complementary probes, followed by their labeling with a protein enzyme for subsequent signal generation and amplification. This has resulted in the detection of attomolar DNA

* Corresponding author. Willem de Croylaen 42, Box 2428, B-3001, Leuven, Belgium.

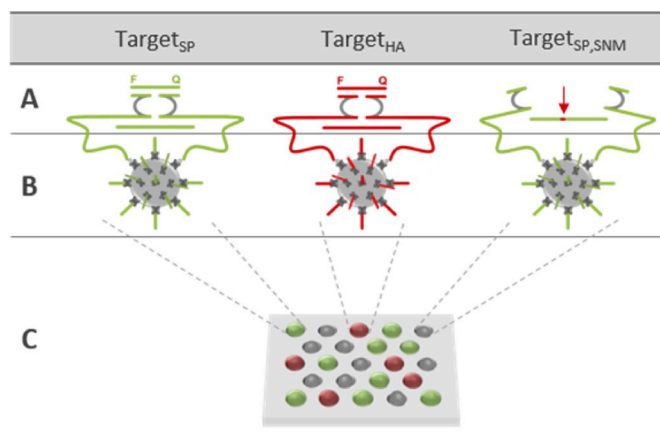
E-mail address: jeroen.lammertyn@kuleuven.be (J. Lammertyn).

¹ Equal contribution.

target concentrations using both a droplet-based microfluidic platform (Guan et al., 2015) and microwell-based platforms. The latter include the SiMoA™ platform (Song et al., 2013) and the more recently described hydrophilic-in-hydrophobic (HIH) microwell array platform (Tripodì et al., 2018), that also enables discrimination of single nucleotide mutations (SNMs). Despite their improvements in terms of erroneous target amplification, these methods are still plagued by the drawbacks associated with using protein enzymes, such as temperature sensitivity and stability, stringent buffer requirements, limited design flexibility and multiplexing potential.

An alternative class of enzymes, so-called NA-based enzymes (NAzymes), have nucleotides as building blocks and as such can withstand more stringent conditions (e.g. pH, temperature) compared to their protein counterparts (Kasprowicz et al., 2017; Nakano et al., 2017; Nesbitt et al., 1999). Moreover, they are highly flexible and have been utilized for different applications, including detection of heavy metals (Wu et al., 2010; Yun et al., 2016; Zhang et al., 2011), NA (Lu et al., 2017; Wang et al., 2018), and pathogens (Ali et al., 2017; Kim et al., 2018; Lee et al., 2017), amongst many others. Remarkably, the 10–23 core NAzymes with an inherent RNA-DNA hybrid cleavage activity (Santoro and Joyce, 1997) are among the most widely studied NAzymes. A first class of these NAzymes, the DNAzyme or deoxyribonucleic acid enzyme, is composed of a conserved catalytic core flanked by adjustable binding arms. These arms bind with the substrate sequence by Watson Crick base-pairing while the catalytic core mediates cleavage of the RNA-DNA hybrid motif in the substrate (Santoro and Joyce, 1997). Another class of NAzymes, derived from DNAzymes, are the multicomponent NAzymes (MNAzymes) (Mokany et al., 2010). MNAzymes are composed of 2 partzymes, each containing one-half of the catalytic core, 1 substrate-binding arm, and 1 additional target-binding arm, enabling formation of the functional enzyme only in the presence of the NA target sequence. This target sequence can be derived from virtually any target entity, hence providing an immense design flexibility to generate a diverse repertoire of NAzymes for a multitude of applications. As such, MNAzymes can be used not only for signal generation and amplification, but they also bear inherent target detection properties (Mokany et al., 2013; Tabrizi et al., 2015). Moreover, the sequence of the substrate-binding arms can also be easily modified to give rise to an even larger number of novel enzymes thus enabling multiplexing (Mokany et al., 2010).

Starting from all the above-mentioned advantages of NAzymes, here we present for the first time a microwell-based bioassay that relies solely on NAzymes for detection of NA targets, signal generation, and signal amplification, without needing protein-based enzymes in any of these steps. Although NAzymes are traditionally used at elevated temperatures, the presented concept operates completely at standard room temperature, thanks to the recently designed 10–23 core NAzymes by our group (Ven et al., 2019). In addition, we demonstrate the potential of this protein-free approach for easy multiplex detection in microwells. This involved designing of 2 MNAzymes to specifically recognize part of the genome from 2 pathogens: the gram positive bacterium *Streptococcus pneumoniae* (SP) and the human adenovirus (HA), a non-enveloped dsDNA virus (both known to colonize the nasopharynx causing serious respiratory tract infections) (Haus et al., 2007). Furthermore, we also successfully show the specificity of the assay for the true target compared to SNMs, in microwells, hereby revealing the single base-pair resolution of this approach at room temperature and in the absence of protein enzymes. To accomplish this and evaluate the sensitivity offered by different platforms, we establish the performance of the MNAzymes first in solution (Scheme 1A), then after being immobilized on superparamagnetic beads (Scheme 1B) and finally in HIH femtoliter-sized microwells (Scheme 1C) (Witters et al., 2013). Considering the clinical relevance of the studied pathogens, we also demonstrate duplex target detection and SNM discrimination from the true target in spiked nasopharyngeal swab samples in the microwell-based platform. This work reveals the enormous potential of bead-based NAzyme biosensors for



Scheme 1. Schematic representation of MNAzyme-based NA detection in 3 different platforms: (A) in solution, (B) on magnetic beads in solution and (C) on magnetic beads in microwell arrays, the latter illustrating the signal, generated in a femtoliter-volume after individual bead seeding and substrate confinement. All MNAzymes comprise the same 10–23 core and have target- and substrate-binding arms, tailored for detection of either the *Streptococcus pneumoniae*-based target (Target_{SP}) or the human adenovirus-based target (Target_{HA}), or discrimination of the *Streptococcus pneumoniae*-based target, carrying an SNM (depicted with red dot and red arrow in Target_{SP,SNM}).

diagnostic purposes, with the future outlook of developing highly flexible and stable digital bioassays with sub-femtomolar detection limits.

2. Materials & methods

2.1. Reagents and NA sequences

Detailed information on the reagents and the sequences of the MNAzymes, targets and substrates used in this study can be found in Supplementary information (S1.1).

2.2. MNAzyme evaluation in solution

Individual detection of Target_{SP} and Target_{HA} in solution was performed in a 25 μ L mixture containing a 5-fold dilution of the target (125 nM, 25 nM, 5 nM, 1 nM) and the corresponding partzymes and substrate at a fixed concentration of 250 nM, all prepared in reaction buffer (10 mM Tris-HCl with 50 mM KCl and 20 mM MgCl₂, pH 8.3). The SNM effect was evaluated at a concentration of 5 nM using Target_{SP,SNM1-6}. Duplex detection of Target_{SP} and Target_{HA} with the same 5-fold dilution for each target (125 - 1 nM) was obtained in a single 25 μ L mix, containing 250 nM partzymes and substrates for both targets. Additionally, duplex control tests were performed by evaluating mixtures containing only 1 target (Target_{SP} or Target_{HA}) at a concentration of 5 nM, in combination with both MNAzymes and both substrate sequences, all at a final concentration of 250 nM. As negative controls, samples without target (0 nM) were included in all the above-mentioned experiments. For readout, the DNA mix was transferred to a 384-well clear-bottom microplate (Glasatelier Saillart, Meerhout, Belgium) and fluorescence was measured every minute for 15 min at standard room temperature, using a SpectraMax iD3 (Molecular Devices LLC, San Jose, USA). For detection of FAM- and HEX-based signals, excitation/emission values were set at 485/535 nm and 529/567 nm, respectively.

All measurements in the manuscript were performed in triplicate, and all samples were stored on ice before readout. The limit of detection (LOD) was calculated as described in Supplementary information (S1.6).

2.3. MNzyme evaluation on beads in bulk

The beads are functionalized with MNzymes as described in Supplementary information (S1.3) and are used to capture Target_{SP} or Target_{HA} at 2-fold dilution (1000–125 pM) in dextran-SSC buffer (5x saline-sodium citrate buffer with 10% dextran sulfate and 0.1% Tween20), and in 10-fold diluted nasopharyngeal swab samples, following description in Supplementary information (S1.4) and based on our previous work (Tripathi et al., 2018). To measure the fluorescence, 10 μ L of the beads were added to 20 μ L of substrate in reaction buffer, at a final concentration of 278 nM, for effective signal generation in a 384-well clear-bottom microplate. Fluorescence was measured every minute for 60 min at 23 °C, using wavelengths as detailed above.

Following the same protocol, detection of Target_{SP,SNM1} was performed at a target concentration of 250 pM whereas duplex detection was evaluated with samples containing both Target_{SP} and Target_{HA}, each at 250 pM. Similar to the experiments without beads, duplex control tests were performed by evaluating complete mixtures containing only 1 target (Target_{SP} or Target_{HA}) at a concentration of 250 pM. For duplex detection, 20 μ L of each of the 10-fold diluted bead populations were added to the samples and for readout, 20 μ L of a mixture of both substrates at a final concentration of 278 nM each, was used. To evaluate the beads carrying only 1 type of partzyme (i.e. partzyme A or partzyme B), the other partzyme was added in excess of the target at a final concentration of 27.8 nM.

2.4. MNzyme evaluation on beads in microwells

A detailed description of the fabrication of the HIH microwells is provided in Supplementary information (S1.4). For singleplex detection, Target_{SP} and Target_{HA} were evaluated at concentrations of 62.5 pM, 31.2 pM, 15.6 pM, 7.8 pM. Detection of Target_{SP,SNM1} (62.5 pM) and duplex detection of Target_{SP} and Target_{HA} (62.5 pM each) was evaluated as described in Supplementary information (S1.5).

The beads, functionalized with partzymes and incubated with the target samples, were subsequently mixed in a 1-to-1 ratio with control beads (i.e. functionalized with partzymes and incubated without (0 pM) the target), unless indicated otherwise. A 5 μ L droplet of this bead mix was positioned on top of the microwell array and manually moved over the array while positioning a permanent magnet (NdFeB, 6 mm diameter, 12.7 N, Supermagnete, Germany) underneath to enable magnet assisted seeding of the beads. After removing the droplet with the remaining beads, 20 μ L of the substrate solution (500 nM, diluted in 10x reaction buffer for optimal signal generation) was added on top of the array and subsequently covered by 180 μ L of PlusOne Drystrip Coverfluid oil. Subsequent removal of the substrate solution from underneath the oil resulted in the generation of sealed, femtoliter-sized reaction wells. For duplex detection, beads were not mixed with control beads, and were confined in the wells with a mixture of both substrates (500 nM each in 10x reaction buffer).

The increase in fluorescence was monitored using an inverted fluorescence microscope and images were analyzed using an in-house developed script (for more details, see Supplementary information, S1.5 and S1.6).

3. Results & discussion

3.1. Validation of MNzyme-based assay in solution for multiplex detection of NA targets and SNM discrimination

To develop a microwell-based bioassay that is completely free of protein-based enzymes, we first adapted 2 existing 10–23 core MNzymes from literature (Mokany et al., 2013) for detecting 2 DNA targets of interest (Target_{SP} and Target_{HA}) and for being performant at standard room temperature. Therefore, the target-binding arms of MNzyme_{SP} and MNzyme_{HA} were designed as complementary sequences to these

targets, respectively. In addition, the substrate-binding arms of both MNzymes and their substrate sequences (Substrate_{SP} and Substrate_{HA}, respectively) were adjusted for the application at standard room temperature as previously described by our group (Ven et al., 2019). Importantly, to enable duplex detection, 2 spectrally distinct fluorophores were incorporated in the 2 substrate sequences, emitting light at a wavelength of 535 nm for Substrate_{SP} and 567 nm for Substrate_{HA}.

The newly designed MNzymes were first tested for their performance in solution. Initially, we evaluated singleplex detection of Target_{SP} and Target_{HA} (125–1 nM at 5-fold dilution, Fig. 1A). Fitting the calibration curves of both targets over the linear range (25–1 nM), resulted in a calculated LOD of 313 ± 23 pM for Target_{SP} and 145 ± 4 pM for Target_{HA}. This demonstrated that both designed MNzymes could successfully detect their specific target sequences at standard room temperature down to pM concentrations. The difference in performance between the different MNzymes, as exemplified by the difference in calculated LOD as well as the difference in slope of the linear fit, are in compliance with previous reports (Mokany et al., 2013). These differences can be attributed to dissimilarity in their target and substrate sequences that affect their base-pair hybridization efficiencies.

Additionally, we also tested the simultaneous detection of both target sequences for the same target concentrations as mentioned above (125–1 nM), using a mixture of the substrates whilst measuring fluorescence emission at both wavelengths (i.e. 535 nm and 567 nm). Here, the calculated LOD for duplex detection was obtained over the same linear range (25–1 nM) and found to be 277 ± 18 pM for Target_{SP} and 602 ± 11 pM for Target_{HA} (Fig. 1B). These findings demonstrated a high specificity of the designed MNzymes for their targets, in both singleplex and duplex settings. In order to further study any non-specific signal arising from cross-reactivity of the MNzymes, additional controls were tested in solution. Here, we used a mixture of both MNzymes, both substrates, and different target combinations, being (1) only Target_{SP}, (2) only Target_{HA}, and (3) both Target_{SP} and Target_{HA}, all at the concentration selected in the middle of the linear dynamic range (i.e. 5 nM). As depicted in Fig. 1C, the negligible fluorescence signal obtained at 535 nm in the presence of Target_{HA} only, and at 567 nm in the presence of Target_{SP} only, demonstrated the lack of non-specific MNzyme activity in the presence of non-complementary targets. Henceforth, the obtained results confirmed that the designed MNzyme system is suited for multiplex NA detection in solution.

Next, we wanted to evaluate the potential of discriminating true target from strands with SNMs. To attain this, we inserted an SNM in the target strand for MNzyme_{SP}, generating Target_{SP,SNM1} (Scheme 1A) and compared the activity of MNzyme_{SP} in the presence of the mutated sequence with the one in the presence of the true target (i.e. Target_{SP}). The experiments were performed in solution at a target concentration of 5 nM, similar to the experiments described in Fig. 1C. As depicted in Fig. 1D, the significantly lower signal in the presence of Target_{SP,SNM1} revealed that the MNzyme does not tolerate the presence of a SNM in the target sequence. Moreover, when evaluating SNMs at alternative locations (Fig. S2), the MNzyme was found to be equally sensitive to mutations adjacent to the other side of the catalytic core but less or almost completely insensitive to mutations at positions more distant from the catalytic core. This suggested that, in the presence of an SNM next to the catalytic core, the MNzyme cannot form its optimal catalytically active conformation and thereby cannot properly cleave the substrate. This knowledge can be applied for a smart design of the target-binding arms of MNzymes in the context of mutation discrimination, i.e. to ensure that known SNMs of interest are positioned next to the catalytic core, at the most mutation-sensitive position. Moreover, contrary to a previous report on the use of MNzymes for mutation detection (Mokany et al., 2010), our system did not require any additional oligonucleotides nor elevated temperatures, rendering it a simpler and more straightforward approach.

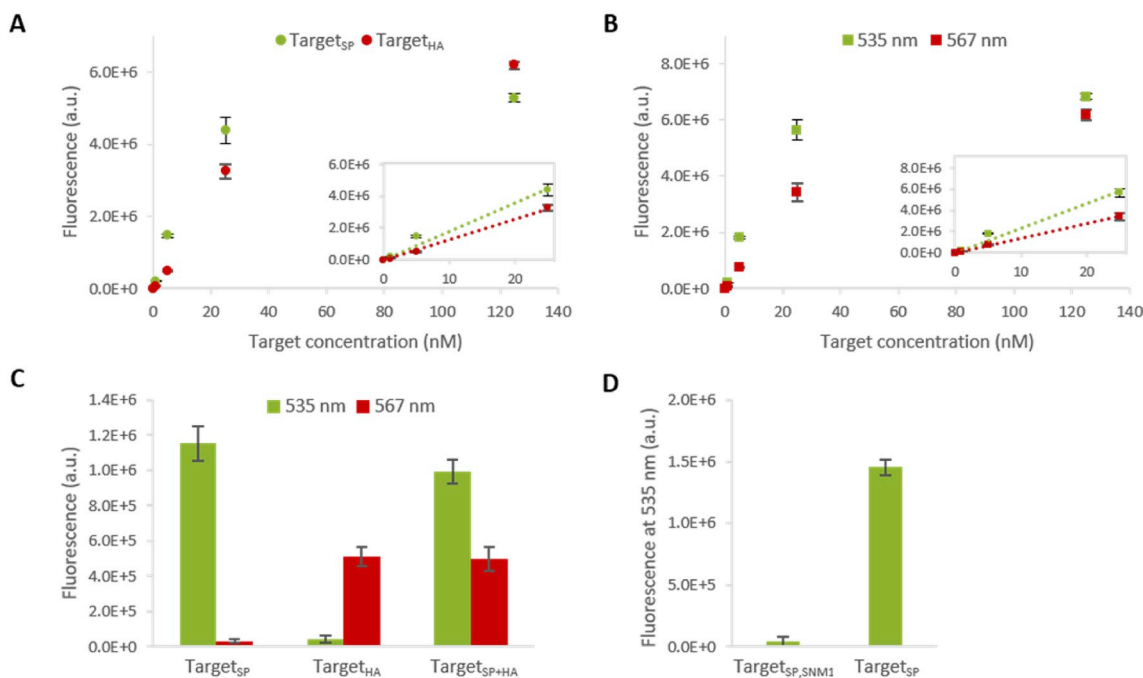


Fig. 1. Performance of the MNazymes in solution at standard room temperature. (A) Detection of Target_{SP} and Target_{tHA} over a 5-fold dilution, ranging from 125 to 1 nM and including a control without target (0 nM) in singleplex (i.e. the reaction mixture comprises either only MNazyme_{SP}, Substrate_{SP} and Target_{SP}, or only MNazyme_{tHA}, Substrate_{tHA}, and Target_{tHA}), with a fluorescent readout at 535 nm for Target_{SP} and 567 nm for Target_{tHA}. The inset shows the linear dynamic range, fitted with an R^2 of 0.972 and 0.996 for Target_{SP} and Target_{tHA}, respectively. (B) Detection of Target_{SP} and Target_{tHA} over a 5-fold dilution, ranging from 125 to 1 nM and including a control without target (0 nM) in duplex (i.e. the reaction mixture comprises a fixed concentration of MNazyme_{SP}, MNazyme_{tHA}, Substrate_{SP}, and Substrate_{tHA} with both the targets added in a 1-to-1 ratio with each other), at both measurement wavelengths. The inset shows the linear dynamic range, fitted with an R^2 of 0.978 and 0.998 for the Target_{SP} and Target_{tHA}, respectively. (C) Evaluation of non-specific signal for duplex detection in the presence of one (Target_{SP} or Target_{tHA}) or both (Target_{SP+HA}) target sequences (5 nM) at both measurement wavelengths. (D) Comparison of the performance of MNazyme_{SP} in the presence of an SNM-carrying target sequence (Target_{SP,SNM1}) and the true target (Target_{SP}) at a 5 nM concentration. For all graphs, the error bars represent the standard deviation of 3 repetitions, after subtraction of the background signal (i.e. the signal from partzymes and substrate, in the absence of target).

3.2. Activity of MNazyme-based bioassay on magnetic beads in solution

To push the designed MNazymes towards their implementation in the HIH microwell-based platform, we tested their activity whilst immobilized on superparamagnetic beads (Scheme 1B). Whereas there are numerous reports on the use of NAzymes on magnetic beads, they either (1) focus on the detection of the metal cofactors of the NAzymes (Huang et al., 2014; Nie et al., 2012; Zhang et al., 2016; Zhuang et al., 2013) instead of NA targets, (2) rely on DNAzymes and hence require additional components or assay steps to enable target detection (Cao et al., 2006; Tram et al., 2014; Willner et al., 2008) and/or (3) are rather complex (i.e. requiring the formation of magnetic nanoparticle assemblies (Tian et al., 2018) or the MNazyme-initiated release of subzymes prior to signal generation (Hasick et al., 2019)). As such, here we report for the first time the use of superparamagnetic beads, functionalized with MNazymes to directly capture the target sequence from the sample. Moreover, we even immobilized both partzyme A and partzyme B from a single MNazyme together on the beads (Scheme 1B), as this approach was found to outperform the system where only 1 biotinylated partzyme (Partzyme A_{SP,bio} or Partzyme B_{SP,bio}) was immobilized on the streptavidin coated beads while the other biotinylated partzyme (Partzyme B_{SP,bio} or Partzyme A_{SP,bio} respectively) was added in solution along with the substrate (Fig. S3). This performance discrepancy can be attributed to the larger diffusion distance to be traversed by the second partzyme in comparison with the situation where both partzymes are immobilized on the beads. This could be counteracted by introducing an additional hybridization step for the partzyme in solution, before the signal generation and readout. However, that would further elongate and complicate the procedure and therefore was not considered in this work.

Using this new approach, the immobilized MNazymes were able to successfully capture their target sequences, Target_{SP} and Target_{tHA}, starting with the lowest concentration detected in solution (1 nM), and going down to 125 pM (Fig. 2A–B). Based on the calibration curve, fitted over the linear range of the measured samples (500 pM to 125 pM), this assay achieved a calculated LOD of 11 ± 1 pM and 21 ± 1 pM for Target_{SP} and Target_{tHA}, respectively. To the best of our knowledge, this is the first report of the combination of low-picomolar NA detection using a bead-based MNazyme assay at room temperature and additionally, it sits competitively amongst the majority of the NAzyme-mediated, bead-based detection methods reported so far (LOD between 10 pM and 100 pM (Cao et al., 2006; Hasick et al., 2019; Niazov et al., 2004)). Moreover, contrary to previous reports on the immobilization of 10–23 DNAzymes on microparticles, where an orientation-dependent inhibition of the catalytic activity was demonstrated (Hasick et al., 2019; Yehl et al., 2012) (i.e. 5' end attachment was found to show higher inhibition levels compared to 3' end attachment, yet lower than combined 5' and 3' end attachment), this orientation-dependent effect was not observed when immobilizing MNazymes on microparticles in this work. This can be attributed to the fact that here we immobilized MNazymes through the target-binding arm, rather than through the substrate-binding arms, as in previous reports (Hasick et al., 2019; Yehl et al., 2012). As such, these results indicate that MNazymes provide, in addition to direct target detection and design flexibility, an added advantage in terms of surface functionalization, which is of great interest for numerous applications in the diagnostics field.

Furthermore, we also evaluated the potential of these MNazyme-functionalized beads for duplex detection. Because the specificity of MNazymes towards different targets and substrates was already proven in solution (Fig. 1), this was done for only one concentration selected in

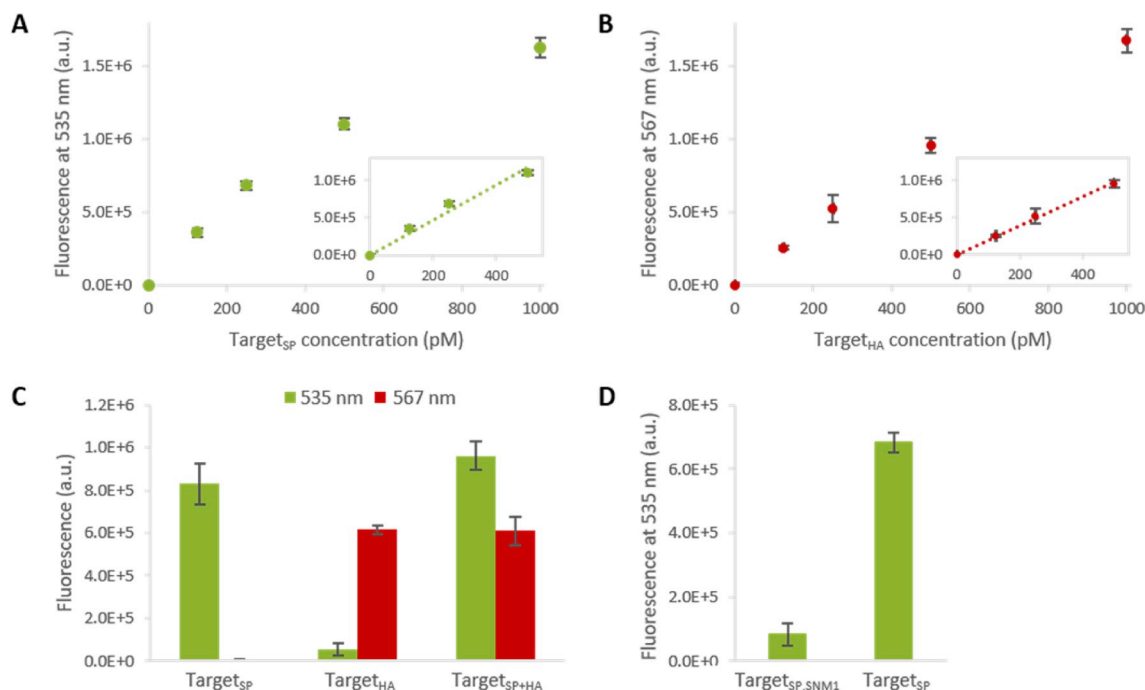


Fig. 2. Performance of the MNazymes on magnetic beads in solution at standard room temperature. (A) Detection of Target_{SP} over a 2-fold dilution, ranging from 1 nM to 125 pM and including a control without target (0 nM), with a fluorescent readout at 535 nm. The inset shows the linear dynamic range, fitted with an R^2 of 0.972. (B) Detection of Target_{HA} over a 2-fold dilution, ranging from 1 nM to 125 pM and including a control without target (0 nM), with a fluorescent readout at 567 nm. The inset shows the linear dynamic range, fitted with an R^2 of 0.996. (C) Evaluation of the non-specific signal for duplex detection in the presence of 1 (Target_{SP} or Target_{HA}) or both (Target_{SP+HA}) target sequences (250 pM) at both measurement wavelengths. (D) Comparison of the performance of MNazyme_{SP} in the presence of an SNM-carrying target sequence (Target_{SP,SNM1}) and the true target (Target_{SP}) at a 250 pM concentration. For all graphs, the error bars represent the standard deviation of 3 repetitions, after subtraction of the background signal (i.e. the signal from partzyme-functionalized beads in the presence of the substrate only).

the middle of the linear dynamic range (250 pM) by incubating a mixture of both targets with a mixture of the 2 bead populations and both substrates. Similar to experiments in solution, control samples with a single target were also included. The bead-based MNazyme assay successfully demonstrated specificity in a duplex detection format, with negligible signal at 535 nm in the absence of Target_{HA} and at 567 nm in the absence of Target_{SP} (Fig. 2C). Also, the ability of this assay to discriminate true target from mutant sequences was proven by using the MNazyme_{SP}-functionalized beads in combination with Target_{SP,SNM1}. As depicted in Fig. 2D, the signal in the presence of the mutant was significantly lower compared with the fully complementary target at a concentration of 250 pM, thereby substantiating the single base-pair resolution of the bead-based MNazyme bioassay for SNMs.

3.3. MNazyme-based singleplex NA detection in microwells

The compatibility of the MNazyme-based bioassay with beads, as demonstrated above, allows for implementation in a myriad of versatile platforms (Guan et al., 2015; Song et al., 2013; Tripodi et al., 2018), thus enabling the development of sensitive bioassays. In this study, we implemented the bead-based MNazyme bioassay on an in-house developed femtoliter-sized, HIH microwell platform (Daems et al., 2019; Pérez-Ruiz et al., 2018; Witters et al., 2013). The target was captured on the MNazyme-functionalized superparamagnetic beads (off-chip), and individual beads were trapped in the microwells with the assistance of a magnet. Next, the MNazyme substrate was added and sealed in the microwells using mineral oil. Upon substrate cleavage by the active, MNazyme-functionalized beads within the confined femtoliter volume of the microwell, there was a localized increase in fluorescence. The latter was subsequently detected via fluorescence microscopy, and the resulting images were processed to acquire the overall, normalized average fluorescence of the wells with active beads using an in-house established image analysis procedure (Fig. S1). Here,

we evaluated a 2-fold dilution range of Target_{SP} (62.5 pM to 7.8 pM), and seeded a 1-to-1 mixture of the beads with target and without target in the microwell array (Fig. 3A). The latter beads were implemented as internal control to correct for variations in well dimensions and illumination between arrays. An example of the obtained microscopy images is depicted in Fig. 3B. As shown in Fig. 3C, a linear trend was observed between 31.2 pM and 7.8 pM Target_{SP}, resulting in a calculated LOD of 180 ± 13 fM. As such, we obtained two orders of magnitude increase in sensitivity from the low picomolar to the femtomolar range when compared to the bead-based bulk assay. This confirmed that a decrease of reaction volume by means of using microwells indeed leads to an increase in assay sensitivity, which can be attributed to the localized, high concentration of fluorescence in the femtoliter-sized well, as previously reported (Walt, 2014). Moreover, here we established for the first time an assay for NA detection in microwells, purely driven by DNA-based enzymes for target detection, signal generation, and signal amplification. This combined action of the MNazyme turns this concept into a highly simple system, requiring only a single target-hybridization step. Hence, this obviates the need of additional incubation steps with detection-probes and enzyme-labels, as previously reported in conventional bead-based assays for NA detection using protein enzymes (Guan et al., 2015; Song et al., 2013; Tripodi et al., 2018). Furthermore, our methodology now outperforms, to the best of our knowledge, all-but-one previously reported NAzyme-based, protein-free assays (LOD ≥ 1.5 pM (Cao et al., 2006; Hasick et al., 2019; Mokany et al., 2010; Niazov et al., 2004; Tian et al., 2018)). Moreover, unlike the best-performing DNAzyme-based system with a LOD of 50 fM (Fu et al., 2009), we obtain sub-picomolar detection limits without involving additional signal amplification strategies (e.g. DNAzyme-functionalized labelling nanoparticles (Fu et al., 2009)). We speculate that these additional amplification approaches would enable to further increase the sensitivity of our method, potentially achieving digital target detection to reach similar detection limits as those

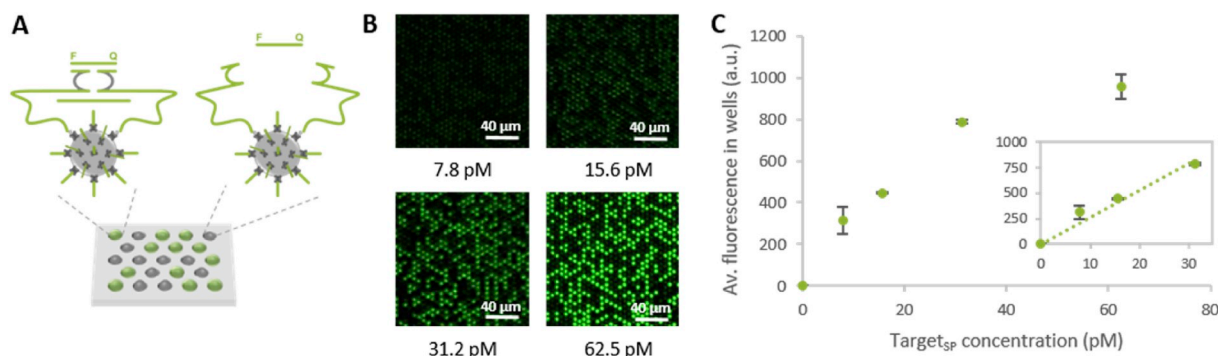


Fig. 3. Performance of MNzyme_{SP} on beads in microwells at standard room temperature. (A) Schematic representation of a concept utilizing 1-to-1 mixture of beads with and without targets in HIH microwells. (B) Fluorescent images of the resulting signal in the microwell arrays for a 2-fold dilution, ranging from 62.5 pM to 7.8 pM, measured with a WIBA filter. The average fluorescence intensity in the wells represents the target concentration. (C) Detection of Target_{SP} over the 2-fold dilution and including a control without target (0 nM). The inset shows the linear dynamic range, fitted with a linear curve ($R^2 = 0.956$). The error bars represent the standard deviation of 3 repetitions, after subtraction of the background signal (i.e. the signal from partzyme-functionalized beads in substrate-sealed wells, in the absence of the target).

previously reported using protein-based digital assays for NA detection (68 aM (Tripodi et al., 2018) to 0.83 fM (Song et al., 2013)), and thus also being competitive with the gold standard PCR techniques (Song et al., 2013).

3.4. Microwell-based multiplex NA detection with single base-pair resolution in nasopharyngeal swabs

Next, we evaluated the potential of multiplex target detection in the microwells using this MNzyme-based bioassay. This was done directly in 10-fold diluted nasopharyngeal swab samples, spiked with Target_{SP} and Target_{HA} (62.5 pM) together, considering (1) the clinical relevance of the studied pathogens for respiratory tract infections and (2) the successful detection of both targets in the bead-based MNzyme assay in 10-fold diluted swabs that demonstrates stability of the system in complex matrix (Fig. S4). For multiplex detection in microwells, the targets were captured on a 1-to-1 mixture of both bead populations, followed by bead seeding and substrate sealing in the microwells (Fig. 4A). As can be seen in Fig. 4B, an increase in fluorescence was observed in the wells with beads carrying Target_{SP} at the emission wavelength for Substrate_{SP}, and for beads with Target_{HA} at the emission wavelength for Substrate_{HA}. As such, we demonstrated for the first time the discrimination of 2 targets simultaneously on this HIH microwell platform. Moreover, this is the first report on microwell-based multiplex target detection without the need for coded bead populations to decode the fluorescent signals, associated with different target molecules, as is the case when relying on the use of a single protein-based enzyme (Rissin et al., 2013). Importantly, our approach is based on the design flexibility of MNzymes which, contrary to protein enzymes, can be easily adjusted to generate a

variety of fluorescent signals upon target-mediated cleavage of a variety of substrates (Mokany et al., 2013). Therefore, this simple approach shows great promise for more extensive multiplexed detection, without the design limitations associated with protein enzymes. Furthermore, the successful multiplex detection of targets, captured from clinically relevant matrix, shows the untapped potential for the development of sensitive, robust, and clinically relevant DNA-driven bioassays.

Lastly, we also wanted to demonstrate that the single base-pair resolution of the MNzyme-based detection system for SNMs can be translated to femtoliter-sized microwells and to another matrix than a buffer. Therefore, we spiked the target (62.5 pM) in 10-fold diluted nasopharyngeal swab samples, incubated it with the beads and, as depicted in Fig. 5A, seeded a 1-to-1 mixture of those beads with beads without target (i.e. internal control as described previously). As depicted in Fig. 5B, a negligible signal was generated in the presence of Target_{SP}, SNM1 compared with the fully complementary Target_{SP}. These results revealed the potential of this bead-based MNzyme bioassay for successful discrimination of mutant strands from true target strands in clinically relevant samples, holding great promise for future application in NA diagnostic assays. Moreover, when compared to a previously reported assay for bead-based discrimination of SNMs in microwells (Tripodi et al., 2018), where a DNA ligase was applied to obtain a mutation-specific assay, the MNzymes' high specificity for target base mutations adjacent to the catalytic core allows for our approach to be highly simplified and protein-enzyme-independent. As such, this concept once more underlines the value of using MNzymes in microwell-based assays for a variety of NA detection principles.

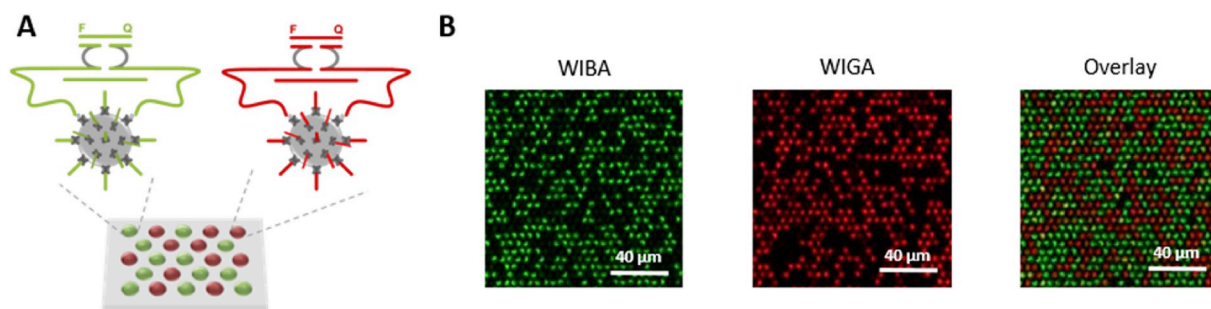


Fig. 4. Multiplex detection using MNzyme_{SP} and MNzyme_{HA} on beads in microwells at standard room temperature in 10-fold diluted nasopharyngeal swab samples. (A) Schematic representation of the signal resulting from the isolation of a 1-to-1 mixture of beads that carry either MNzyme_{SP} and Target_{SP} or MNzyme_{HA} and Target_{HA}, for multiplex detection. (B) Fluorescent images of the resulting signal in the microwell arrays for the duplex detection of Target_{SP} and Target_{HA} (62.5 pM), measured with a WIBA and WIGA filter, respectively, and visualized together via an overlay image.

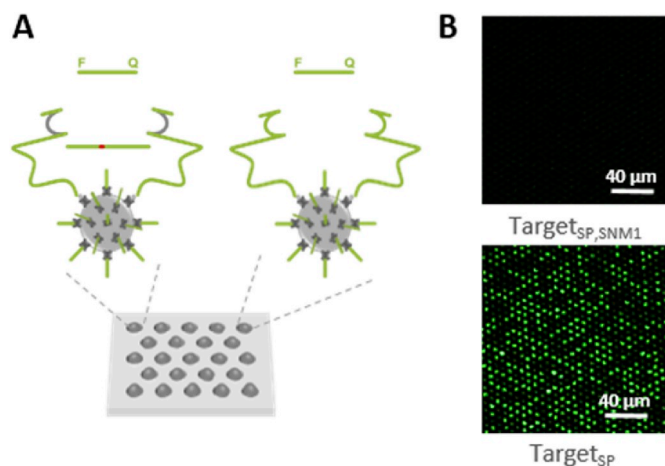


Fig. 5. Performance of MNzyme_{SP} in the presence of an SNM-carrying target sequence (Target_{SP,SNM1}) on beads in microwells at standard room temperature in 10-fold diluted nasopharyngeal swab samples. (A) Schematic representation of the signal resulting from the isolation of a 1-to-1 mixture of beads with Target_{SP,SNM1} and without target. (B) Fluorescence images of the signal in the microwell arrays for the detection of Target_{SP,SNM1} and, as a positive control, Target_{SP} (performed as in Fig. 3A), both at a target concentration of 62.5 pM and measured with a WIBA filter.

4. Conclusion

Here we report, for the first time, a purely NA-driven bioassay for the detection of NA targets in femtoliter-sized microwells and, moreover, at standard room temperature. In addition to singleplex detection we demonstrated that this approach enables a straightforward duplex detection, and revealed its single base-pair resolution. To achieve this, we reported a double hat-trick, where (1) target recognition, (2) signal generation, and (3) signal amplification all rely on a single MNzyme, as validated (1) in solution, (2) on beads in solution and (3) on beads in femtoliter-sized microwells. In solution, the MNzymes demonstrated successful detection of their respective NA targets, both in singleplex assay (with calculated LOD of 313 ± 23 pM and 145 ± 4 pM for Target_{SP} and Target_{HA}, respectively) and in duplex assay (LOD of 277 ± 18 pM and 602 ± 11 pM for Target_{SP} and Target_{HA}, respectively), the latter emphasizing that the designed MNzyme system was suited for multiplex NA detection in solution. The observed differences in performance between 2 designed MNzymes can be explained with the effect that different target and substrate sequences have on their base-pair hybridization efficiencies and are in agreement with previous reports (Mokany et al., 2013). Whilst immobilized on beads, MNzymes successfully captured Target_{SP} or Target_{HA}, achieving a calculated LOD of 11 ± 1 pM and 21 ± 1 pM, respectively, and as such being comparable to the majority of the NAzyme-mediated, bead-based detection methods reported so far. Subsequently, this MNzyme-based bioassay was successfully implemented in HIH femtoliter-sized microwells, resulting in sub-picomolar detection limits (calculated LOD of 180 ± 13 fM) for Target_{SP}, rendering it the most sensitive MNzyme-based bioassay that does not rely on secondary amplification strategies, as reported so far. Lastly, the microwell-based approach also effectually enabled duplex detection, relying on the design flexibility of MNzymes to obtain multiple fluorescent signals rather than using coded beads, and discrimination of SNMs from true target strands without the need of complex assay configurations, all in diluted nasopharyngeal swab samples. These findings allow for future integration with multiple platforms, including digital bioassays with single-molecule resolution, providing promising avenues to further exploit this DNA-powered NA detection technique.

Declaration of competing interest

The authors declare that they have no known competing financial interests or personal relationships that could have appeared to influence the work reported in this paper.

Acknowledgements

This work has received funding from Research Foundation–Flanders (FWO SB/1S30116N, FWO SB/1SC8519N, FWO SB/1S30016N, FWO G084818N) and the European Union's Horizon 2020 research and innovation programme under the Marie Skłodowska-Curie grant agreement No 675412 (H2020-MSCA-ITN-ND4ID) and No 764281 (H2020-MSCA-ITN-AiPBAND). The nasopharyngeal swabs were kindly provided by the Laboratory of Medical Microbiology of the Vaccine and Infectious Disease Institute of the University of Antwerp.

Appendix A. Supplementary data

Supplementary data to this article can be found online at <https://doi.org/10.1016/j.bios.2020.112017>.

References

- Abe, A., Kajiyama, N., Kawaguchi, R., Inoue, K., Kato, J., Kohara, M., Yoshida, M., Tanaka, T., Tanaka, S., 1999. Quantitation of hepatitis B virus genomic DNA by real-time detection PCR. *J. Clin. Microbiol.* 37, 2899–2903.
- Ali, M.M., Brown, C.L., Jahanshahi-Anbuhi, S., Kannan, B., Li, Y., Filipe, C.D.M., Brennan, J.D., 2017. A printed multicomponent paper sensor for bacterial detection. *Sci. Rep.* 7, 12335.
- Borst, A., Box, A.T.A., Fluit, A.C., 2004. False-positive results and contamination in nucleic acid amplification assays: suggestions for a prevent and destroy strategy. *Eur. J. Clin. Microbiol. Infect. Dis.*
- Cao, Z., Li, Z., Zhao, Y., Song, Y., Lu, J., 2006. Magnetic bead-based chemiluminescence detection of sequence-specific DNA by using catalytic nucleic acid labels. *Anal. Chim. Acta* 557, 152–158.
- Daems, D., Rutten, I., Bath, J., Decrop, D., van Gorp, H., Pérez Ruiz, E., De Feyter, S., Turberfield, A.J., Lammertyn, J., 2019. Controlling the bioreceptor spatial distribution at the nanoscale for single molecule counting in microwell arrays. *ACS Sensors* ascensors.9b00877.
- de Abreu Fonseca, C., Teixeira, M.M.G., Romero, E.C., Tengan, F.M., da Silva, M.V., Shikanai-Yasuda, M.A., 2006. Leptospira DNA detection for the diagnosis of human leptospirosis. *J. Infect.* 52, 15–22.
- Fu, R., Li, T., Park, H.G., 2009. An ultrasensitive DNAzyme-based colorimetric strategy for nucleic acid detection. *Chem. Commun.* 5838–5840.
- Guan, W., Chen, L., Rane, T.D., Wang, T.-H., 2015. Droplet digital enzyme-linked oligonucleotide hybridization assay for absolute RNA quantification. *Sci. Rep.* 5, 13795.
- Han, X., Wang, J., Sun, Y., 2017. Circulating tumor DNA as biomarkers for cancer detection. *Genom. Proteom. Bioinform.* 15, 59–72.
- Hasick, N.J., Ramadas, R., Todd, A.V., 2019. Subzymes: regulating DNAzymes for point of care nucleic acid sensing. *Sens. Actuators B Chem.* 297, 126704.
- Haus, U.-U., Klamt, S., Stephen, T., 2007. Computing knock out strategies in metabolic networks. *Lancet Infect. Dis.* 4, 144–154.
- Heim, A., Ebnet, C., Harste, G., Pring-Åkerblom, P., 2003. Rapid and quantitative detection of human adenovirus DNA by real-time PCR. *J. Med. Virol.* 70, 228–239.
- Huang, X., Hao, Y., Wu, H., Guo, Q., Guo, L., Wang, J., Zhong, L., Lin, T., Fu, F., Chen, G., 2014. Magnetic beads based colorimetric detection of mercuric ion. *Sens. Actuators B Chem.* 191, 600–604.
- Kasprovicz, A., Stokowa-Sojtyk, K., Jeżowska-Bojczuk, M., Wrzesiński, J., Ciesiolka, J., 2017. Characterization of highly efficient RNA-cleaving DNAzymes that function at acidic pH with no divalent metal-ion cofactors. *ChemistryOpen* 6, 46–56.
- Kim, S.U., Batule, B.S., Mun, H., Shim, W.-B., Kim, M.-G., 2018. Ultrasensitive colorimetric detection of Salmonella enterica Typhimurium on lettuce leaves by HRPzyme-integrated polymerase chain reaction. *Food Control* 84, 522–528.
- Kishine, M., 2014. Loop-mediated isothermal amplification. *Nippon Shokuhin Kagaku Kogaku Kaishi* 61, 100, 100.
- Kühnemund, M., Hernández-Neuta, I., Sharif, M.I., Cornaglia, M., Gijls, M.A.M., Nilsson, M., 2017. Sensitive and inexpensive digital DNA analysis by microfluidic enrichment of rolling circle amplified single-molecules. *Nucleic Acids Res.* 45, gkw1324.
- Lee, J., Jung, J., Lee, C.S., Ha, T.H., 2017. Design and optimization of an ultra-sensitive hairpin DNA aptasensor for Salmonella detection. *RSC Adv.* 7, 34933–34938.
- Lu, X., Shi, X., Wu, G., Wu, T., Qin, R., Wang, Y., 2017. Visual detection and differentiation of Classic Swine Fever Virus strains using nucleic acid sequence-based amplification (NASBA) and G-quadruplex DNAzyme assay. *Sci. Rep.* 7, 44211.
- Mokany, E., Bone, S.M., Young, P.E., Doan, T.B., Todd, A.V., 2010. MNzymes, a versatile new class of nucleic acid enzymes that can function as biosensors and molecular switches. *J. Am. Chem. Soc.*

- Mokany, E., Tan, Y.L., Bone, S.M., Fuery, C.J., Todd, A.V., 2013. MNAzyme qPCR with superior multiplexing capacity. *Clin. Chem.* 59, 419–426.
- Nakano, S., Horita, M., Kobayashi, M., Sugimoto, N., 2017. Catalytic activities of ribozymes and DNazymes in water and mixed aqueous media. *Catalysts* 7, 355.
- Nesbitt, S.M., Erlacher, H.A., Fedor, M.J., 1999. The internal equilibrium of the hairpin ribozyme: temperature, ion and pH effects. *J. Mol. Biol.* 286, 1009–1024.
- Niazov, T., Pavlov, V., Xiao, Y., Gill, R., Willner, I., 2004. DNzyme-functionalized Au nanoparticles for the amplified detection of DNA or telomerase activity. *Nano Lett.* 4, 1683–1687.
- Nie, D., Wu, H., Zheng, Q., Guo, L., Ye, P., Hao, Y., Li, Y., Fu, F., Guo, Y., 2012. A sensitive and selective DNzyme-based flow cytometric method for detecting Pb²⁺ ions. *Chem. Commun.* 48, 1150–1152.
- Pérez-Ruiz, E., Decrop, D., Ven, K., Tripodi, L., Leirs, K., Rosseels, J., van de Wouwer, M., Geukens, N., De Vos, A., Vanmechelen, E., Winderickx, J., Lammertyn, J., Spasic, D., 2018. Digital ELISA for the quantification of attomolar concentrations of Alzheimer's disease biomarker protein Tau in biological samples. *Anal. Chim. Acta* 1015, 74–81.
- Rissin, D.M., Kan, C.W., Song, L., Rivnak, A.J., Fishburn, M.W., Shao, Q., Piech, T., Ferrell, E.P., Meyer, R.E., Campbell, T.G., Fournier, D.R., Duffy, D.C., 2013. Multiplexed single molecule immunoassays. *Lab Chip* 13, 2902–2911.
- Santoro, S.W., Joyce, G.F., 1997. A general purpose RNA-cleaving DNA enzyme. *Proc. Natl. Acad. Sci.* 94, 4262–4266.
- Schneider, A., Kraus, H., Schuhmann, R., Gissmann, L., 1985. Papillomavirus infection of the lower genital tract: detection of viral DNA in gynecological swabs. *Int. J. Cancer* 35, 443–448.
- Song, L., Shan, D., Zhao, M., Pink, B.A., Minnehan, K.A., York, L., Gardel, M., Sullivan, S., Phillips, A.F., Hayman, R.B., Walt, D.R., Duffy, D.C., 2013. Direct detection of bacterial genomic DNA at sub-femtomolar concentrations using single molecule arrays. *Anal. Chem.* 85, 1932–1939.
- Tabrizi, S.N., Tan, L.Y., Walker, S., Poljak, M., Twin, J., Garland, S.M., Bradshaw, C.S., Fairley, C.K., Mokany, E., 2015. Multiplex assay for simultaneous detection of Mycoplasma Genitalium and macrolide resistance using pass MNAzyme QPCR. *Sex. Transm. Infect.* 91, A36.
- Tian, B., Han, Y., Wetterskog, E., Donolato, M., Hansen, M.F., Svedlindh, P., Strömberg, M., 2018. MicroRNA detection through DNzyme-mediated disintegration of magnetic nanoparticle assemblies. *ACS Sens.* 3, 1884–1891.
- Tram, K., Kanda, P., Salena, B.J., Huan, S., Li, Y., 2014. Translating bacterial detection by DNazymes into a litmus test. *Angew. Chem. Int. Ed.* 53, 12799–12802.
- Tripodi, L., Witters, D., Kokalj, T., Huber, H.J., Puers, R., Lammertyn, J., Spasic, D., 2018. Sub-femtomolar detection of DNA and discrimination of mutant strands using microwell-array assisted digital enzyme-linked oligonucleotide assay. *Anal. Chim. Acta* 1041, 122–130.
- Ven, K., Safdar, S., Dillen, A., Lammertyn, J., Spasic, D., 2019. Re-engineering 10–23 core DNA- and MNAzymes for applications at standard room temperature. *Anal. Bioanal. Chem.* 411, 205–215.
- Vincent, M., Xu, Y., Kong, H., 2004. Helicase-dependent isothermal DNA amplification. *EMBO Rep.* 5, 795–800.
- Walt, D.R., 2014. Protein measurements in microwells. *Lab Chip* 14, 3195–3200.
- Wang, R., Wang, L., Xu, X., Jiang, W., 2018. An enzyme-free and label-free fluorescence biosensor for microRNA detection based on cascade amplification of DNzyme-powered three-dimensional DNA walker and hybridization chain reaction. *Sens. Actuators B Chem.* 268, 287–292.
- Warwick, S., Wilks, M., Hennessy, E., Powell-Tuck, J., Small, M., Sharp, J., Millar, M.R., 2004. Use of quantitative 16S ribosomal DNA detection for diagnosis of central vascular catheter-associated bacterial infection downloaded from. *J. Clin. Microbiol.* 42, 1402–1408.
- Willner, I., Cheglakov, Z., Weizmann, Y., Sharon, E., 2008. Analysis of DNA and single-base mutations using magnetic particles for purification, amplification and DNzyme detection. *Analyst* 133, 923.
- Witters, D., Knez, K., Ceysens, F., Puers, R., Lammertyn, J., 2013. Digital microfluidics-enabled single-molecule detection by printing and sealing single magnetic beads in femtoliter droplets. *Lab Chip* 13, 2047.
- Wu, C.S., Khaing Oo, M.K., Fan, X., 2010. Highly sensitive multiplexed heavy metal detection using quantum-dot-labeled DNazymes. *ACS Nano* 4, 5897–5904.
- Yehl, K., Joshi, J.P., Greene, B.L., Dyer, R.B., Nahta, R., Salaita, K., 2012. Catalytic deoxyribozyme-modified nanoparticles for RNAi-independent gene regulation. *ACS Nano* 6, 9150–9157.
- Yun, W., Cai, D., Jiang, J., Zhao, P., Huang, Y., Sang, G., 2016. Enzyme-free and label-free ultra-sensitive colorimetric detection of Pb²⁺ using molecular beacon and DNzyme based amplification strategy. *Biosens. Bioelectron.* 80, 187–193.
- Zhang, H., Lin, L., Zeng, X., Ruan, Y., Wu, Y., Lin, M., He, Y., Fu, F., 2016. Magnetic beads-based DNzyme recognition and AuNPs-based enzymatic catalysis amplification for visual detection of trace uranyl ion in aqueous environment. *Biosens. Bioelectron.* 78, 73–79.
- Zhang, X.-B., Kong, R.-M., Lu, Y., 2011. Metal ion sensors based on DNazymes and related DNA molecules. *Annu. Rev. Anal. Chem.* 4, 105–128.
- Zhuang, J., Fu, L., Xu, M., Zhou, Q., Chen, G., Tang, D., 2013. DNzyme-based magneto-controlled electronic switch for picomolar detection of lead (II) coupling with DNA-based hybridization chain reaction. *Biosens. Bioelectron.* 45, 52–57.